

# A novel linear virtual temperature constructing method for thermal error modeling of machine tools

Chengxin Zhang<sup>1,2</sup> · Feng Gao<sup>1</sup> · Zhenhua Meng<sup>3</sup> · Bohan Zhao<sup>1</sup> · Yan Li<sup>1</sup>

Received: 16 November 2014 / Accepted: 19 April 2015 / Published online: 1 May 2015  
© Springer-Verlag London 2015

**Abstract** When a thermal error model of a machine tool is established, selecting the appropriate temperature measurement point is a very difficult problem. This paper proposes a novel method for constructing a linear virtual temperature. The proposed method can overcome the problem of selecting the temperature measurement point. First, temperature-thermal expansion hysteresis characteristics are used to divide the temperature measurement points into two groups. Each temperature variable is then chosen through a principal component analysis (PCA). Finally, using two temperature-variable weights and the correlative coefficient thermal displacement as the maximum optimal indexes, two temperature-weighted coefficients are calculated, and a linear virtual-temperature variable related to the thermal error linearity is then formed. In establishing the proposed thermal error model, the linear virtual temperature formed can serve as a system input variable. The proposed method was tested on a three-axis milling machine to determine the spindle Z-axial thermal error, and the results show that the root mean square error (RMSE) is reduced by 11 % and the sum of the squares of the error (SSE) is reduced by 39 % in comparison with a direct application of a temperature variable when establishing such a model. In the proposed method, only two temperature measurement points are used to establish a model, through which

the complexity in determining the optimal measurement points through a traditional method, along with the number of temperature measurement points required, is greatly reduced.

**Keywords** Machine tools · Thermal error · Hysteresis characteristic · Linear virtual temperature · PCA

## 1 Introduction

At present, the manufacturing industry requires a very high accuracy in machine part machining. The thermal error has become the major factor affecting machine tool processing [1]. There are two general approaches to decreasing or even eliminating the influence of thermal errors: hardware compensation methods and software compensation methods to control over them [2, 3].

Software compensation methods are currently popular research areas owing to their flexible and convenient applications [3]. A software compensation of the thermal errors is used to elucidate the relationship between the thermal errors and temperature in a machine tool. Before a highly accurate thermal error compensation model can be established, it is necessary to solve a key problem in selecting the appropriate temperature measurement points on the machine tool. Accordingly, the selection of temperature measurement points is a key function for the accuracy and robustness of the thermal error model. To obtain the appropriate temperature measurement points, scholars have put forward the following methods:

1. Mathematical statistics method

The common advantages of the existing mathematic statistics method include the following: a large number

✉ Chengxin Zhang  
qfzcx\_sd@163.com

Feng Gao  
gf2713@126.com

<sup>1</sup> School of Mechanical and Precision Instrument Engineering, Xi'an University of Technology, Xi'an 710048, China

<sup>2</sup> Qufu Normal University, Rizhao 276826, China

<sup>3</sup> Yantai University, Yantai 264005, China

of sensors can be arranged on a machine tool, and several optimal measurement points can then be selected from the arranged sensors through a statistical analysis [4–12]. However, there are certain disadvantages of this type of method: (1) it takes a great deal of time to arrange a large number of sensors on a machine tool based solely on experience, and it is thus necessary to search for the optimal measurement points through the application of an algorithm. (2) The temperature sensor arrangement is unlikely to cover the optimal positions, resulting in certain omissions. (3) The optimal positions are unlikely to be adaptable for a layout of the temperature sensors. Finally, (4) different statistical theories are likely to obtain different results for sensors of the same group. These above issues are likely to cause the optimal measurement points to be unattainable.

## 2. Numerical calculation method

To carry out an analysis using a numerical calculation method, a finite element method (FEM) and a finite difference method (FDM) are mainly adopted [13, 14]. The advantages of a numerical calculation method are a complete computer simulation with low cost. The disadvantages of a numerical calculation method are an inability to provide accurate boundary conditions when a simulation is carried out. In addition, the effects of the joint surfaces among the different parts of a machine tool can lead to errors in the simulation results.

## 3. Theoretical analysis method

Ma [15] generated an analysis of a mechanism produced using the thermal expansion hysteresis behaviors, and accounted for the changing laws when measuring the points on the temperature-thermal expansion curves for different distances from the thermal resources, that is, the measurement distance to the thermal resources ranges from nearby to far away, and thus, the curves can gradually change from concave to convex. He suggested that, to increase the

accuracy of a thermal error model, the positions of the temperature sensors selected should appear to have a linear relation with the thermal expansion. In addition, the work in [15] indicates that the optimal measurement point of a one-dimensional rod part should be on  $x_{\text{opt}} = 0.5632\sqrt{kt/c_p}$ . Accordingly, although this method is used to carry out a theoretical analysis of the optimal measurement points, the analysis model applied may neglect the influence of the heat exchanges through a convection current, thereby affecting the accuracy; in addition, on the machine tool parts may be no way to directly use the given formula to arrange the temperature sensors. Although the hysteresis characteristic has a negative effect on the accuracy of the model, it can be used to classify or select the temperature measurement points. For example, in [16], the optimal temperature measurement points are selected using the hysteresis characteristic.

To avoid neglecting the optimal temperature measurement points when using a mathematical statistics method and the hysteresis characteristic to classify such points, this research provides an optimal method for determining virtual measurement points using the temperature-thermal expansion hysteresis ability for a classification of the temperature variables and a linearity formation. When the temperature measurement points are classified, it can be determined whether their layout should be adjusted to make certain that their positions are relatively rational. When the pre-arranged temperature sensors are not at linear measurement positions, one temperature sequence appearing to have a linear relation with the thermal expansion is structured from two temperature sequences that are not in the best position in terms of the measurement point of the temperature-thermal expansion curve. The structured temperature sequence is known as the linear optimal virtual temperature. This temperature is the optimal value under the best indices of the temperature-thermal expansion linearity. The advantage of this method is that there are only two temperature measurement points needed to structure a single linear temperature-thermal expansion sequence. This can provide a favorable condition for the later establishment of a thermal error model, particularly simplifying the mathematic model such that only a small amount of calculations is required, thereby meeting the real-time needs of various application fields.

## 2 Analysis of linear virtual temperature structure theory and test

### 2.1 Performance experiment on the rod part of a temperature-thermal expansion

The basic reason for the existence of thermal expansion hysteresis characteristics is that the thermal conduction velocity is smaller than the expansion velocity, thus making the temperature point at different positions and the end thermal expansion curves form different shapes. In the following stage, an analysis of the linear optimal measurement points should be conducted to select the best positions. To decrease the analysis complexity, the thermal conduction process of one-dimensional rods is used in the examples to carry out the analysis, as shown in Fig. 1. The rod length is 1 m in natural convection condition. Eleven temperature sensors are arranged on the rod in order from the left as  $T_0, T_1, \dots, T_{10}$ . The distance between each sensor is 10 cm. The thermal resource strength is  $1000 \text{ W/m}^2$ . At the rod end, eddy current sensors are installed to monitor the thermal distortion. After the temperature rises for 2 h and falls for 1 h, the temperature-thermal expansion curves are measured, as shown in Fig. 2 (the curves after  $T_5$  are too close to be marked in the figure).

It can be seen from Fig. 2 that during the temperature increase stage, the  $T_0$  temperature measurement point is nearer the thermal resource, the temperature change is faster than the varying thermal expansion, and thus the curves displayed are rendered in a concave shape; as the temperature sensor becomes increasingly distant from the thermal resource, the concavity of the curve gradually decreases. For instance, at the  $T_2$  position, the temperature-thermal expansion curve gradually becomes approximately linear. At the  $T_3$  point, which is farther from the thermal resource, the temperature-thermal expansion curve becomes convex, thus illustrating that the thermal expansion becomes faster than the temperature variation, but on the curves displaying that temperature change is smaller while thermal variation is larger. This indicates that, with the changes in the distance between the temperature measurement point and the position of the thermal resource, the shape of the temperature-thermal expansion curve also happens to change gradually. The curve shape from the nearby to far away temperature measurement points gradually changes from concave to convex. Based on the above situation, there

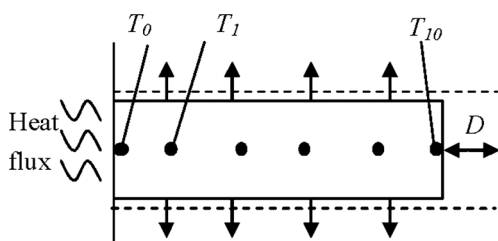


Fig. 1 Arrangement of sensors on a rod

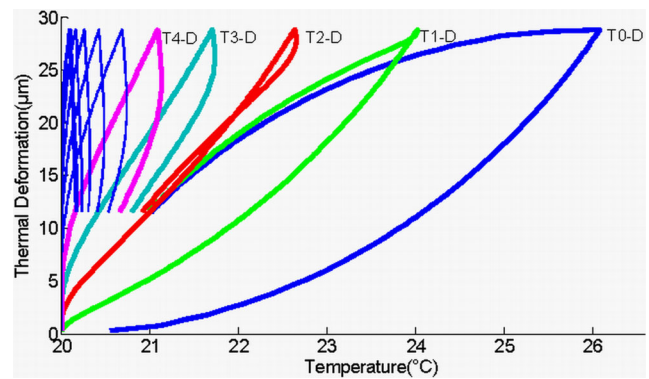


Fig. 2 Sketch of temperature-thermal error relation

is bound to be certain positions where the temperature-thermal expansion test curve can be approximately linear, for example, at the  $T_2$  position. The above description is an intuitive analysis of the temperature increase stage. It can be determined from the fundamental theorem of calculus that when the second derivative of one curve is larger than zero, the curve is concave; when the second derivative is smaller than zero, the curve is convex; and when the second derivative is equal to zero, the curve becomes a straight line. Accordingly, based on the symbols of the second derivative curve and in combination with the shape features of the temperature thermal expansion curve, the following conclusions can be obtained: when the measurement point is farther from the thermal resource, the second derivative of the temperature-thermal expansion curve is smaller than zero, and when the measurement point is near the thermal resource, the second derivative of the temperature expansion is equal to zero. Based on the above conclusion, the relations between the distance of the measurement point and thermal resource can be determined in accordance with the magnitude of the second derivative of the temperature-thermal expansion curves. At the same time, the temperature measurement points can be divided into two groups in accordance with the positive and negative values of the second derivative of the temperature-thermal expansion curves: (1) when the second derivative of the temperature-thermal curve is smaller than zero, the temperature measure point is located on the right side of the linear temperature measurement point, and (2) when the second derivative of the temperature-expansion curve is larger than zero, the temperature measurement point is located on the left side of the linear temperature measurement point. Based on the above principle, it is easy to classify the temperature measurement points. The physical aspect of this method is definite and easy to implement and overcomes the weak points of the unclear physical aspects of the classification of the temperature measurement points determined through a statistical analysis and miscellaneous calculations.

Because the distances between the temperature measurement points and the thermal resource positions differ, the

temperature-thermal expansion curves have different characteristics. To ensure the prediction accuracy of a thermal error model, Yang [17] suggested that a dynamic thermal error model method should be established to improve the model prediction accuracy. To further improve the prediction accuracy of the thermal error model, Yang [18] also suggested that an integrated recurrent neural network model can adapt to the non-linearity and non-statistical performances during the thermal deformation process, thereby further improving the accuracy of the model prediction. Although these two types of thermal error models have greatly improved the accuracy of thermal error prediction, their structures are complicated and inconvenient for practical use. If the temperature measurement points are correctly at the linear temperature measurement points, a linear thermal error model that is simple in structure, and with high prediction accuracy, can be established. For this reason, Ma [15] suggested that when a thermal error model is established for a machine tool, the best temperature measurement points should be selected for those points that have a linear relation with the thermal expansion, and the author provided a formula for calculating the linear position. However, because the structure of a machine tool is very complicated and irregular, it is not easy to carry out a calculation directly though the linear point formula given in [15]. Therefore, a hypothesis was suggested: If the temperature measurement points are not at the linear points, can a temperature sequence appearing to have an approximately linear relation with the thermal expansion of a machine tool be structured through several different points? The next section analyzes this question.

## 2.2 Structure and analysis of linear virtual temperature

Through the analysis described in Section 2.1, we are able to carry out a classification and determination of the temperature measurement points based on their distance from the thermal resources in terms of the shape of the temperature-thermal expansion curve at certain points. For a convenient and practical application in structuring the linear temperature measurement points, a simply hypothesis is put forward, i.e., if there are two temperature measurement points, the shape of the measured temperature-thermal expansion curve for the increasing temperature stage will be convex, and the for the opposite, it will be concave; in addition, the temperature sequences structured through these two measurement points appear to have a linear relation with the thermal expansion, i.e., there is a single linear temperature measurement point.

The following proves the existence of a single virtual linear measurement point through the two measurement points mentioned above. The above topic can be described through mathematic language: based on the fact that the second derivative of  $f_1(x)$  is smaller than zero and that the second derivative of  $f_2(x)$  is larger than zero, a single function,  $f(x)$ , can be

structured through the weighted sum of  $f_1(x)$  and  $f_2(x)$  so as to make the second derivative zero, as shown in Fig. 3.

Proof: To begin, assume that there exists a second derivative of  $f(x)$ .

Assuming that the function,  $f(x)$ , is structured through a weighted  $f_1(x)$  and  $f_2(x)$ , and making the second derivative be equal to zero, then

$$f(x) = af_1(x) + bf_2(x), \quad (1)$$

where  $a$  and  $b$  are weighted coefficients satisfying  $a+b=1$ .

To seek the second derivative for two sides of Eq. (1) and letting  $f''(x)=0$ , we obtain

$$af_1''(x) + bf_2''(x) = 0, \quad (2)$$

where  $f_1''(x)<0, f_2''(x)>0$ , and  $a+b=1$ . We can then have the following equation:

$$a = \frac{f_2''(x)}{f_2''(x)-f_1''(x)}. \quad (3)$$

Owing to the fact that the signs of the second derivatives  $f_1(x)$  and  $f_2(x)$  are the opposite and their denominators are not equal to zero so that Eq. 3 exists, the conclusion is proved that is to assign the weighted coefficients in terms of Eq. 3 as able to weight two functions to structure the function as the linear.

Through the above proof, one temperature sequence appearing to have a linear relation with the thermal expansion can be structured through a temperature-thermal expansion curve appearing to be a convex and concave temperature sequence for two measurement points. In the previous section, the temperature measurement points were derived into two groups in terms of their thermal expansion hysteresis behaviors. Accordingly, when structuring the virtual measurement points, as long as one convex sequence and one concave two-temperature sequence of the temperature-thermal expansion curves are chosen, a single virtual measurement point can be structured. Because many temperature measurement points are arranged during these measurements, many kinds of combined methods exist. To make the most out of the effects of such a combination, it is necessary to solve the problem of how to select two temperature variables required from the

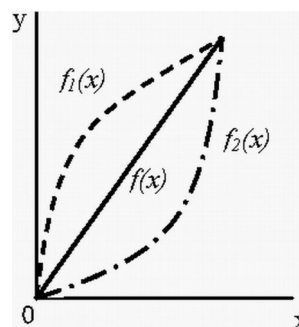


Fig. 3 Sketch diagram of the linear function of a structure

temperature measurement points of two groups so as to create a combination with the best results.

### 2.3 Main principle of a PCA

When certain objects are studied, many indexes or variables should always be taken into account to reflect the characteristics and laws of the objects in a comprehensive and accurate manner. Accordingly, because as many indexes as possible can be considered to accurately reveal the objective characteristics and laws, a problem may be generated in which the more indexes that are considered, the more complicated the analytical process will become. For this reason, Hotelling [19] suggested the use of a principal component analysis (PCA). Details of this analysis method can be found in [20]. The purpose of a PCA is to study how a few variables are used to account for the original variables when expressing information through several linear combinations of the original variables under the prerequisite of losing less information. In this way, we can achieve the objective of playing a role in reducing the number of dimensions and simplifying the problem under the prerequisite of retaining the original information. The abstracted comprehensive indexes are called the principal components, the characteristics of which are as follows:

1. Every principal component is a linear combination of each original variable.
2. The number of principal components is much smaller than the number of original variables.
3. The principal components have reserved most of the information regarding the original variables.
4. There are no correlations among each principal component.

### 2.4 Temperature variable selection

When the temperature variables are selected, the more information carried by the temperature sequence that is available, the more effective the results of the established model will be. The PCA method is used to abstract the first and second components from the information matrix formed by all of the temperature variables, and a correlation analysis is conducted from the first and second principal components. The two maximum temperature variables of the correlative coefficients of the first and second principal components serve as two temperature variables to structure the linear virtual temperature.

One point needs to be explained: Why are the principal components directly used as virtual temperature variables? The main reason is that every principal component is part of the original variable linear combination. For the arrangement of the sensors, there is no reduction in their number, and thus, the principal components are directly used to structure the

temperature sequence without a reduction in the number of sensors. If the correlation coefficients of the selected temperature variables and the principal component are larger, it can be ensured that the information provided by the temperature variables will be the same or similar to the principal component.

### 2.5 Structure method of linear virtual temperature

Through the PCA, we selected two temperature variables from numerous temperature variables with an aim to structure a variable with the thermal expansion value appearing to have a linear relation through the two variables. The structured temperature cannot strictly become a linear relation owing to the cause of the measurement error. For this reason, only the maximum variable of the linear correlation coefficient can be constructed. This problem can be converted into an optimal constraint problem.

$$\begin{aligned} & \text{Max}(\text{corrcoef}(T, Z)) \\ \text{s.t. } & T = a_1 \cdot T_1 + a_2 \cdot T_2, \\ & a_1 + a_2 = 1 \end{aligned} \quad (4)$$

where  $T$  is the structured temperature,  $Z$  is the thermal expansion,  $T_1$  and  $T_2$  are the temperature variables selected using the PCA method,  $a_1$  and  $a_2$  are variable coefficients, and  $\text{corrcoef}()$  is the correlation function.

Equation (4) is an extreme condition value problem, where the two variable coefficients  $a_1$  and  $a_2$  can be easily obtained using Lagrange's method of multipliers.

Summarizing the above description, a linear virtual temperature flow chart is shown in Fig. 4.

### 2.6 Linear virtual temperature structure tests

An experiment was carried out to test the effectiveness of the structural linear virtual temperature suggested in this research. The 11 temperature measurement points are arranged on a one-dimensional thermal conducting rod in order, as shown in Fig. 1. The measured temperature-thermal expansion curves are shown in Fig. 2. It can be seen in Fig. 2 that at all temperature measurement points, temperature  $T_2$ , has the best linear relation with thermal expansion  $D$ . If the linear correlation coefficients between the constructed virtual temperature variable and thermal expansion sequence can be equal to or greater than that between measurement temperature  $T_2$  and thermal expansion sequence, the validity of the method of contracture linear virtual temperature variables can be verified.

It can be seen from Fig. 2 that the temperature variables can be divided into two groups to satisfy the arrangement requirements of the temperature measurement points. As the structural flow chart in Fig. 4 shows, for the third step, all of the

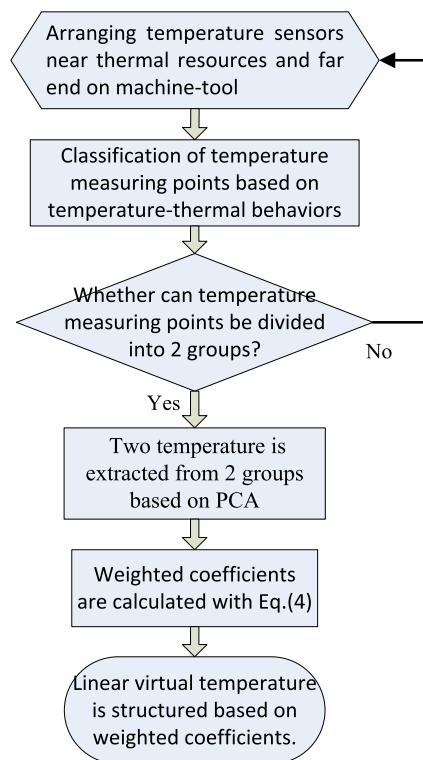


Fig. 4 Structure of a linear virtual temperature flow

temperature variables can be used to structure an information matrix, and the first and the second principal components of the information matrix can then be calculated. The maximum temperature variable with a similar coefficient as the first principal component is  $T_1$ , with the similar coefficient being 0.9775. The maximum temperature variable with a similar coefficient as the second principal component is  $T_6$ , with the similar coefficient being 0.9774. These two temperature variables have one convex and one concave thermal expansion curve, respectively, which satisfies the prerequisite conditions for structuring linear virtual measurement points. The weighted coefficients of the two temperature variables are calculated using Eq. (4). The weighted coefficient of  $T_1$  is 0.256 and that of  $T_6$  is 0.744. Accordingly, the linear virtual temperature is

$$T = 0.256 * T_1 + 0.744 * T_6.$$

The correlation coefficient of virtual temperature  $T$  and the thermal expansion sequence is 0.9995, whereas the correlation coefficient of the  $T_2$  variable and the thermal expansion sequence for the measurement temperature is 0.9967. It can be seen from this contrast that the structured virtual temperature and linearity of the thermal expression are quite high, as shown in Fig. 5.

Through the contrast in the correlation data and Fig. 5, the temperature sequence and thermal expansion sequence obtained through the method used for structuring the virtual

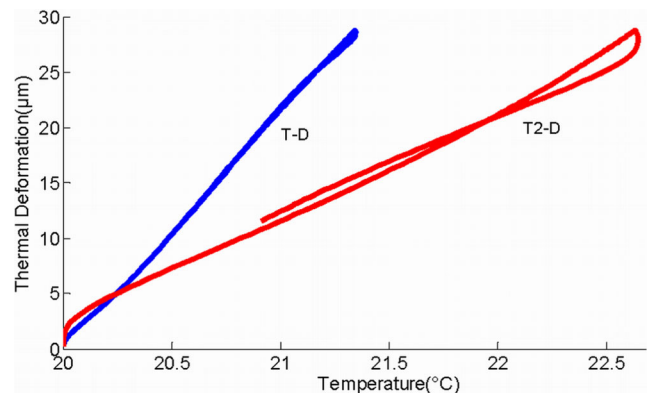


Fig. 5 Effect of structure on the linear virtual temperature

temperature have a very good linear relation with each other. The above description has proved the effectiveness of this method.

### 3 Application example

#### 3.1 Selection of temperature measurement points and model construction

In Section 2, the effectiveness of this method was tested for a simple case. In the following, the structure of the virtual temperature method suggested in this paper is further tested on real machine tools. An experiment was carried out on a milling machine with a tri-axial numerical control. The model for the Z-shaft axial thermal error was established. Four temperature sensors,  $T_1$ ,  $T_2$ ,  $T_3$ , and  $T_4$ , were arranged on the spindle bearings to monitor changes in the temperature. An eddy sensor,  $D$ , was installed on the spindle end part to monitor the axial error, as shown in Fig. 6. The spindle was in operation for 120 min at 1000 r/min. The room temperature was 22.3 to 23.5 °C. Small fluctuations could be considered as constants. The amount of temperature change and variations in the thermal expansion are shown in Fig. 7. The relation between the amount of temperature change at each measurement point and the variations in the thermal expansion are shown in Fig. 8. Based on an analysis of structuring the linear virtual temperature described in Section 2, measurement points  $T_2$ ,  $T_3$ , and  $T_4$  could be finalized into one group, and  $T_1$  could be another group on its own.

Based on the structural linear virtual temperature sequence method suggested in this paper, first, four temperature variables can be used to structure one information matrix, and the first and second main components of the matrix are then calculated to obtain the maximum temperature variable with a similar coefficient, i.e., 0.998, as the first main component,  $T_1$ . The maximum temperature variable with a similar coefficient,

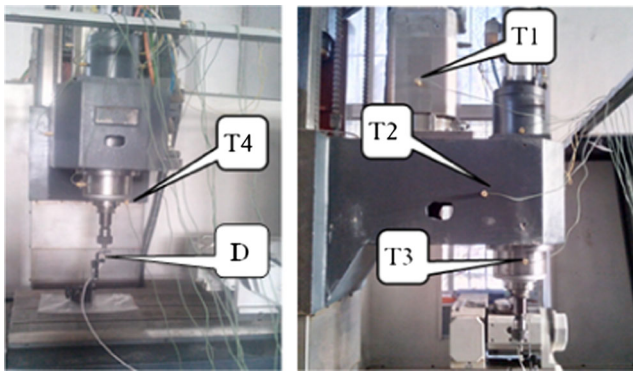


Fig. 6 Arrangement of sensors on the machine tool

i.e., 0.9203, as the second main component is  $T_4$ . Two temperature-sequence-weighted coefficients are calculated using Eq. (4). The weighted coefficient of  $T_1$  is 0.438, and that of  $T_4$  is 0.562. To verify the effectiveness of the virtual measurement point, the multiple linear regression model is used to compare the forecast effect of the different input variables [7]. Therefore, the virtual temperature  $T_{14}$  structured by  $T_1$  and  $T_4$  should be

$$T_{14} = 0.438 * T_1 + 0.562 * T_4.$$

The first-order polynomial model is established based on the virtual temperature,  $T_{14}$ , and thermal expansion,  $D$ :

$$D_1 = 3.404 * T_{14} - 3.284. \tag{5}$$

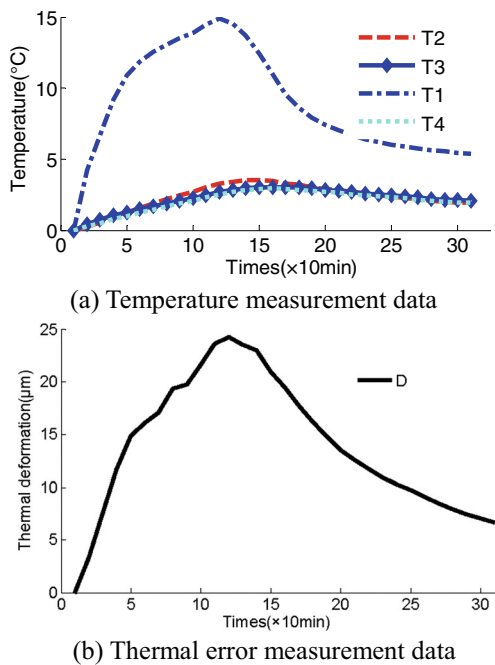


Fig. 7 Measurement data. a Temperature measurement data. b Thermal error measurement data

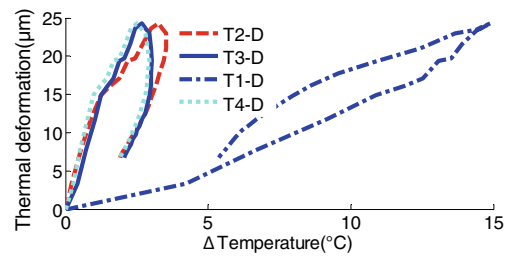


Fig. 8 Temperature-thermal expansion relations

To compare the accuracy of the virtual structural temperature sequence method, all of the temperature variables are adopted to establish the polynomial model.

$$D_2 = 15.711 * T_2 + 16.3989 * T_3 + 0.3747 * T_1 - 30.3562 * T_4 \tag{6}$$

In addition,  $T_1$  and  $T_4$  can be directly used to establish the regression polynomial thermal error model.

$$D_3 = 1.3407 * T_1 + 1.1132 * T_4 \tag{7}$$

The above-three established models are called model I, model II, and model III for convenience in a later comparison.

### 3.2 Model tests

In Section 3.1, the spindle Z-axis thermal error model is established. What is the effect of the model prediction? It is still necessary to change the operation conditions to carry out the tests. The sensor position should be arranged as shown in Fig. 6. The spindle should first be in operation for 120 min at 900 r/min, and then stop operating for 40 min to lower the temperature. Next, the spindle is put into operation again for 40 min at 1100 r/min, and then stops its operation. The amount of temperature change at the measurement points and the thermal expansion curves are shown in Figs. 9 and 10, respectively.

The tested data are placed into the three models to fit the effects, as shown in Fig. 11. Here,  $Z$  is the thermal expansion data of the spindle. The residual indexes of each model are shown in Table 1.

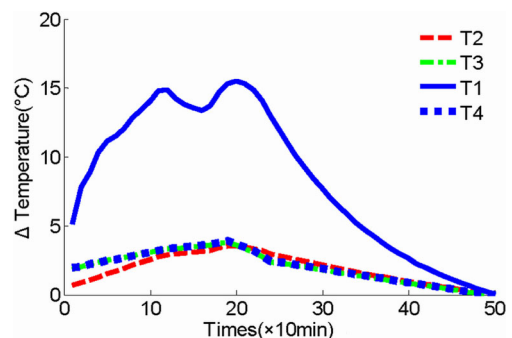
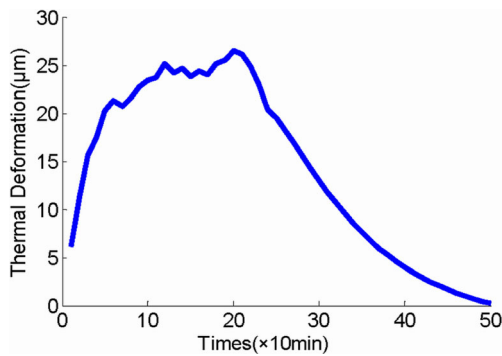
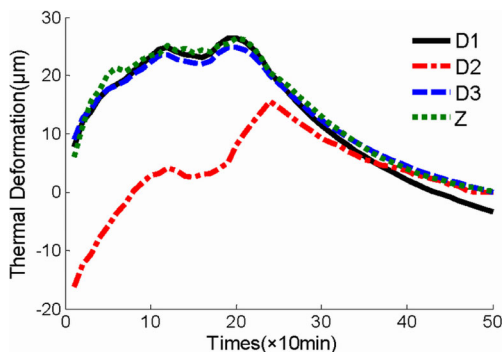


Fig. 9 Temperature measurement data



**Fig. 10** Thermal error measurement data

It can be seen from Fig. 11 that when all of the temperature variables are adopted, the prediction effects of model II are the poorest. The main reason for this is that the introduction of more variables can increase the measurement noise, thereby generating the poor model results. It can be seen from Fig. 11 that, by structuring virtual temperature variable model I and directly adapting temperatures 1 and 4 to establish model III, the prediction results are comparatively close. It can be seen from the data comparison in Table 1 that, although model I and model III had the same input variables, the different treatments of the temperature variables caused the prediction accuracy of model I to be superior to that of model III, for example, the root mean square error (RMSE) was reduced by 11 %, and the sum of the squares of the error (SSE) was reduced by 39 %. For the same model structure and order, this experiment illustrates that the model established through the structuring of the linear virtual temperature method has the highest accuracy. The main reason for this is that, when two temperature variables are weighted, the information of the two variables cannot be completely entered into the model, but are determined based on the size of the weighted coefficient, whereas the weighted coefficient is determined based on the optimal guidance or standard of the linear degree of the temperature-thermal expansion, and thus the application of the virtual temperature of the structure in the model



**Fig. 11** Comparison of model building

**Table 1** Comparison of the predicted residual results of three models under the same input data ( $\mu\text{m}$ )

Modeling method	RMSE	Max residual	SSE
Model I	0.9686	2.8063	51.6678
Model II	8.8937	26.2438	10514
Model III	1.0935	3.0241	75.9121

establishment is superior to the direct application of two temperature variables.

## 4 Conclusions

With an aim at structured linear virtual temperature variables when modeling the thermal error of a machine tool, this paper studied the measurement point classification, key temperature variable abstraction, and method of structuring the linear virtual measurement points. The following conclusions were obtained through an analysis and experimentally:

1. Through an analysis of the temperature-thermal expansion hysteresis characteristics, a classification method was proposed to classify the temperature measurement points, that is, the convex curve of the temperature-thermal expansion hysteresis characteristics can be one group and those of the concave curve can be another group;
2. The application of a PCA allows two key temperature variables carrying the most information to be selected from the temperature variables of the two groups. The information carried by the two temperature variables can account for the majority of information provided by all of the temperature variables. When the model is established, only these two temperature variables are needed.
3. The two temperature variables selected through a weighted combination allow a temperature sequence appearing to have an approximately linear relation with the thermal expansion to be obtained.

**Acknowledgments** This study is supported by the National Natural Science Foundation of China (no. 51375382) and Shaanxi Province Office of Education to serve the local program (no. 2013JC27).

## References

1. Ramesh R, Mannan M, Poo A (2003) Thermal error measurement and modelling in machine tools: Part I. Influence of varying operating conditions. *Int J Mach Tools Manuf* 43(4):391–404
2. Li J, Zhang W, Yang G, Tu S, Chen X (2009) Thermal-error modeling for complex physical systems: the-state-of-arts review. *Int J Adv Manuf Technol* 42(1):168–179



3. Mayr J, Jędrzejewski J, Uhlmann E, Alkan Donmez M, Knapp W, Hartig F, Wendt K, Moriawaki T, Shore P, Schmitt R (2012) Thermal issues in machine tools. *CIRP Ann Manuf Technol* 61(2):771–791
4. Lo C-H, Yuan J, Ni J (1999) Optimal temperature variable selection by grouping approach for thermal error modeling and compensation. *Int J Mach Tools Manuf* 39(9):1383–1396
5. Lee J-H, Yang S-H (2002) Statistical optimization and assessment of a thermal error model for CNC machine tools. *Int J Mach Tools Manuf* 42(1):147–155
6. Yang JG, Ren YQ, Liu GL, Zhao HT, Dou XL, Chen WZ, He SW (2005) Variable selecting and modeling of thermal errors on an INDEX-G200 turning center. *Int J Adv Manuf Technol* 26(7–8):814–818
7. Han J, Wang L, Wang H, Cheng N (2012) A new thermal error modeling method for CNC machine tools. *Int J Adv Manuf Technol* 62(1–4):205–212
8. Yang H, Ni J (2005) Adaptive model estimation of machine-tool thermal errors based on recursive dynamic modeling strategy. *Int J Mach Tools Manuf* 45(1):1–11
9. Zhang T, Ye WH, Liang RJ, Lou PH, Yang XL (2013) Temperature variable optimization for precision machine tool thermal error compensation on optimal threshold. *Chin J Mech Eng* 26(1):158–165
10. Li YX, Yang JG, Gelvis T, Li YY (2008) Optimization of measuring points for machine tool thermal error based on grey system theory. *Int J Adv Manuf Technol* 35(7–8):745–750
11. En-ming M, Ya-yun G, Lian-chun D, Ji-chao M (2014) Temperature-sensitive point selection of thermal error model of CNC machining center. *Int J Adv Manuf Technol* 74(5–8):681–691
12. Wang H, Wang L, Li T, Han J (2013) Thermal sensor selection for the thermal error modeling of machine tool based on the fuzzy clustering method. *Int J Adv Manuf Technol* 69(1–4):121–126
13. Zhu J, Ni J, Shih AJ (2008) Robust machine tool thermal error modeling through thermal mode concept. *J Manuf Sci Eng Trans ASME* 130(6):61006
14. Xia C, Fu J, Xu Y, Chen Z (2014) Machine tool selected point temperature rise identification based on operational thermal modal analysis. *Int J Adv Manuf Technol* 70(1–4):19–31
15. Ma Y (2001) Sensor placement optimization for thermal error compensation on machine tools. University of Michigan
16. Mian N, Fletcher S, Longstaff A, Myers A (2012) An efficient offline method for determining the thermally sensitive points of a machine tool structure. In *Proceedings of the 37th International Matador Conference*, Springer
17. Yang H, Ni J (2003) Dynamic modeling for machine tool thermal error compensation. *J Manuf Sci Eng Trans ASME* 125(2):245–254
18. Yang H, Ni J (2005) Dynamic neural network modeling for nonlinear, nonstationary machine tool thermally induced error. *Int J Mach Tools Manuf* 45(4):455–465
19. Hotelling H (1933) Analysis of a complex of statistical variables into principal components. *J Educ Psychol* 24(6):417
20. Jolliffe I (2005) *Principal component analysis*. Wiley Online Library